SAND2000-0311C

Role of Alumina Phase and Size in Tungsten CMP

David J. Stein
Sandia National Laboratories, M.S. 1084, P.O. Box 5800, Albuquerque, NM, 87123
(505)-845-8476 dstein@sandia.gov

Robert Y.-S. Her
Ferro Electronic Materials, Ferro Corporation, 1789 Transelco Dr., Penn Yan, NY, 14527

Abstract

The role of the alumina particle phase and size on polish rate and process temperature was studied to elucidate removal mechanisms involved in tungsten CMP using potassium iodate-based slurries. Additional work including polishing of blanket PETEOS and titanium films, and polishing of M1 to V1 to M2 electrical test structures was performed to determine the performance of the various aluminas in production CMP. The polish rate of tungsten was highest with alpha alumina. Delta/theta and gamma alumina showed lower polish rates. Tungsten and PETEOS polish rates increased with particle size. Only alpha alumina was able to clear the titanium barrier stack. The size of the alpha alumina did not effect the electrical characteristics of short loop electrical test structures.

Experimental Description

150 mm diameter Si wafers were used in this work. Blanket PETEOS films were grown by PECVD on bare silicon wafers in an Applied Materials P5000. The blanket titanium films were sputter grown onto blanket PETEOS films using a Varian M2000. The 10 kÅ blanket tungsten films were deposited using a Genus 8720 CVD reactor after an *in-situ* clean. A pre-polish process was performed on the as-deposited tungsten films to eliminate error in the 4-point probe thickness measurements caused by as-deposited film roughness. This process consists of a 30 second polish using baseline slurry. The surface roughness (R_a) of the tungsten film after the pre-polish step was less than 2nm over a 25 μm^2 area as determined by atomic force microscopy (AFM). AFM images and profiles were obtained with a Digital Instruments VX200 AFM profiling AFM.

CMP was performed using an IPEC Avanti 472 polisher. Material removal occurred on the primary platen, which was covered by a K-grooved IC-1400 polyurethane pad (Rodel Corporation, Newark, Delaware). The pad surface process temperature during processing was measured using an IR probe aimed at the center of the wafer track just at the exit from the wafer carrier. The polished wafer then underwent a DI water buff on the second platen, which was covered by a Politex pad (Rodel Corporation). The wafers were cleaned using a double-sided brush scrub process with dilute ammonia on an OnTrak DSS-200. Finally, the wafers were decontaminated with a 15 second dip in 49% HF diluted with 100 parts of DI water. We have previously determined that neither the post-CMP DI water buff, scrub, and decontamination processes remove any material or damage the tungsten surface. Polish rates were determined using pre- and post-CMP 17 site 4-point probe resistivity measurements.

Three phases of alumina (alpha, delta/theta, and gamma) and three sizes of each phase (approximately 0.1 to 0.3 μm) were provided by Ferro Corporation. Wafers were polished with each alumina using a full factorial, four center point replicate DOE (12 runs) in polish pressure and rotation rate. The rotation rate of the platen was matched with the carrier speed to ensure that the velocity between the pad and the wafer was uniform for all points on the wafer surface. All of the slurries used consisted of identical chemistry- 0.1 M potassium iodate buffered to approximately pH 4 using 0.05 M potassium hydrogen phthalate (PHP). The alumina solids content for each slurry was 5% by weight.

Results and Discussion

Figure 1 shows the tungsten polish rate (PR) for each slurry as a function of the product of the polish pressure (P) and relative velocity (v). The solid lines represent the best fit of the model

$$PR = \frac{k'Pv}{(1+k''Pv)} \qquad (1)$$

which is described elsewhere[1]. Table 1 gives the phase of each alumina, the median particle size, and the R^2 values for fits to the polish rate data using both the Preston equation

DISCLAIMER

DISCLAIMER

Portions of this document may be illegible in electronic image products. Images are produced from the best available original document.

$$PR = KPv \quad (2)$$

and Equation 1. Previous results[2] have shown that at high solids and chemistry concentrations the Preston equation fits tungsten CMP data better than data obtained from slurries with lower solids and chemistry concentration. Equation 1, however, fits tungsten CMP data better than the Preston Equation over the entire range of solid and chemistry concentrations. Figures 2, 3, and 4 show polish rate contour plots created from models derived from statistical analysis of the raw data using RS/1 (Domain Solutions Corporation). The contour plots show calculated polish rates at a fixed particle size of 0.1925 μm. The figures clearly show that the polish rate is not a linear function of pressure and velocity. The figures also show that at any given pressure and velocity the alpha alumina has a higher polish rate than either delta/theta or gamma alumina. The polish rates of delta/theta and gamma alumina are similar in the region of polish pressure and velocity studied.

Figure 5 shows the process temperature recorded for each alumina as a function of the product of P and v. The process temperature increases with P and v, which is the same trend seen in previous work[2]. The process temperature was also modeled using RS/1. The model predictions are shown in Figure 2, 3, and 4 for a fixed particle size of 0.1925 μm. The process temperature at any given pressure and velocity does not vary significantly between the alumina phases for the fixed particle size. Further analysis over the particle size range studied (see below) shows that the size of alpha alumina does not have an effect on the process temperature, while the particle size of delta/theta and gamma alumina does have a significant effect on the process temperature. Figure 6 shows the actual (not modeled) process temperature for the experimental centerpoints of pressure and velocity. The data is plotted as a function of the measured particle size. For the data shown process temperature is highest for alpha alumina at the smaller particle sizes but similar for all three phases at the larger particle sizes.

Figure 7 shows the main effects of pressure, velocity, and particle size on polish rate and process temperature. The main effects were calculated using RS/1. There are two important features to this plot. First, particle size is important for each response with the exception of process temperature during CMP using alpha alumina. Second, the order of importance of the factors for each response for each alumina phase is pressure, velocity, and finally particle size.

Subsequent experiments were run to determine the performance of these aluminas in polishing patterned device wafers. A metal 1 (M1) to via 1 (V1) to metal 2 (M2) short loop process was run using a mask set solely designed for back-end electrical testing[3]. The details of the test structures are given elsewhere[4]. These electrical test wafers were run several months after the data described above was collected. The alumina suspensions aged during this period of time so verification of the blanket film polish rates was made. Verification of which slurries would polish through titanium, the hardest of the two metals in the barrier stack to polish, was also made. The results are shown in Table 2. Commercial alumina- and potassium iodate-based tungsten slurry (MSW2000, Rodel Corporation) was used as a baseline for comparison. Figures 8, 9, and 10 show comparisons between the tungsten polish rates of the fresh and the aged aluminas. The polish rate decreased with aging. No visible changes in the alumina suspensions (stored without the additional chemistry in the slurry) were noted during the storage time.

Only the three alpha alumina-based slurries were able to polish through the blanket titanium film. The smallest alpha alumina particle did not polish completely through the film in the time allotted. There were only 12 electrical test wafers. Based upon the ability of each alumina to polish through the titanium film, 4 splits of three wafers each were chosen. The four splits used the baseline slurry, and Ferro SRS187, SRS188, and SRS189 based-slurries. The experimental Ferro alumina suspensions were mixed with the potassium iodate and potassium hydrogen phthalate chemistry described above to make the polish slurry.

In addition to the blanket tungsten, blanket titanium, and patterned wafers, blanket PETEOS was also polished to investigate the oxide polish rate and defects created by the tungsten CMP process. Table 3 shows the data obtained from the blanket PETEOS wafers. The polish rate increases with particle size for the Ferro alumina-based slurries. The Tencor 6200 light point defects (LPD) do not follow a simple linear trend with particle size. The LPD counts were significantly higher for the Ferro alumina-based slurries than for the baseline slurry. The differences seen between the Ferro alumina-based slurries and baseline may be due to the nature of the proprietary particulate(s) or chemistry of the baseline slurry.

Figure 12 shows AFM images of W plugs polished with the slurries described above. The baseline and SRS187-based slurries show small formation of tungsten studs with no tungsten keyholes or corrosion. SRS188- and SRS189-based slurries show more planar tungsten and oxide surfaces, however, some tungsten keyholes are present. None of the slurries show appreciable dishing. Figure 11 shows the

erosion step height, measured by long range (several mm) AFM profiles of the surface, from a 4 mm x 4 mm sea of tungsten plugs to a 4 mm x 4 mm field of oxide. SRS187-based and baseline slurries show more erosion than SRS188- and SRS189-based slurries.

Figures 13, 14, 15, and 16 show the electrical test results as absolute values and die yield for each wafer run with each slurry. Yield is defined as the percentage of structures within 3 sigma of the mean of all similar structures on the wafer. The Figures indicate that there were no significant differences between the electrical properties of the devices formed by the four tungsten CMP slurries.

Summary and Conclusions

Tungsten CMP polish rates and process temperatures using slurries consisting of different types of alumina colloids were studied. The slurry chemistry consisted of 0.1 M potassium iodate and 0.05 M potassium hydrogen phthalate. The alumina used in each slurry was either alpha, delta/theta, or gamma. Three sizes of each phase were used. Tungsten polish rates and process temperatures were reported. The polish rate data fit a previously reported[2] heuristic model better than the Preston equation. Statistical analysis of the data indicates that all three factors (pressure, velocity, and size) of each alumina phase effect the polish rate. Polish pressure and velocity had the greatest effects on both polish rate and process temperature. The particle size had a significantly smaller effect on both responses. Aging of the alumina suspensions decreased the blanket tungsten polish rates. Blanket films of titanium could only be polished using alpha alumina. The blanket PETEOS polish rate increased with alumina particle size. There was no clear trend in light point defects on blanket PETEOS with alumina particle size. Alpha alumina particle size did not effect the electrical performance of the patterned wafers studied.

Acknowledgments

The authors wish to thank Kim Glidden, Claire Parker-Harston, and Dave Shingledecker for processing and equipment support. We would also like to thank Digital Instruments, and especially Tim Cunningham, for use of the VX200 profiling AFM, which was operated by Thomas Gaffney. The authors also wish to thank Marta Verhoff and Dale Hetherington, both of Sandia, for useful discussions.

The majority of this work was performed at Sandia National Laboratories, Albuquerque, New Mexico. This work was partially supported by the United States Department of Energy under contract DE-AC04-94AL85000. Sandia is a multi-program laboratory operated by Sandia Corporation, a Lockheed Martin Company, for the United States Department of Energy.

Table 1: the polish rate model fits (Figure 1) are shown for each alumina. The labels refer to Ferro Corporation's lot number of each alumina.

Alumina	Phase	Size (μm)	Preston Fit R^2	Equation X Fit R^2
SRS189	alpha	0.14	0.98	0.99
SRS188	alpha	0.18	0.98	0.99
SRS187	alpha	0.25	0.98	0.98
SRS186	delta/theta	0.13	0.94	0.95
SRS185	delta/theta	0.18	0.80	0.83
SRS184	delta/theta	0.21	0.97	0.97
SRS183	gamma	0.13	0.92	0.94
SRS182	gamma	0.19	0.94	0.96
SRS181	gamma	0.30	0.92	0.96

Table 2 shows the tungsten polish rate and performance on titanium for each slurry.

Slurry	Slurry Name	Phase	Particle size (μm)	W polish rate (Å min-1)	Std. Dev polish rate (Å min-1)	Cleared 2000 Å Ti in 2 minutes?
1	Baseline	mostly alpha	0.150	2824.4	19.2	Yes
2	SRS183	gamma	0.131	1020.9	181.9	No
4	SRS182	gamma	0.194	1456.8	47.0	No
7	SRS181	gamma	0.299	1445.7	6.4	No
8	SRS186	delta/theta	0.134	1258.9	78.2	No
10	SRS185	delta/theta	0.175	1520.8	91.2	No
9	SRS184	delta/theta	0.213	1513.6	30.6	No
3	SRS189	alpha	0.140	2473.8	31.9	Partial
6	SRS188	alpha	0.179	2670.4	31.5	Yes
5	SRS187	alpha	0.245	3030.7	48.5	Yes

Table 3 shows the results from blanket PETEOS CMP using the alumina-based slurries.

Slurry	Slurry Name	Phase	Particle size (μm)	PETEOS polish rate (Å min-1)	Std. Dev. polish rate (Å min-1)	LPD	LPD Std. Dev.
1	Baseline	mostly alpha	0.150	377.3	2.3	3123.7	1204.9
3	SRS189	alpha	0.140	192.6	5.7	24608.0	2109.5
6	SRS188	alpha	0.179	404.2	9.7	18436.0	341.8
5	SRS187	alpha	0.245	670.2	10.8	30437.7	31.6

[1] D. J. Stein, D. L. Hetherington, and J. L. Cecchi, *The Journal of the Electrochemical Society* **146** (5), 1934, May, 1999.
[2] D. J. Stein, D. L. Hetherington, and J. L. Cecchi, *The Journal of the Electrochemical Society* **146** (1), 376, January, 1999.
[3] Designed by Keith Yoneshige, Sandia National Laboratories.
[4] Please contact the authors.

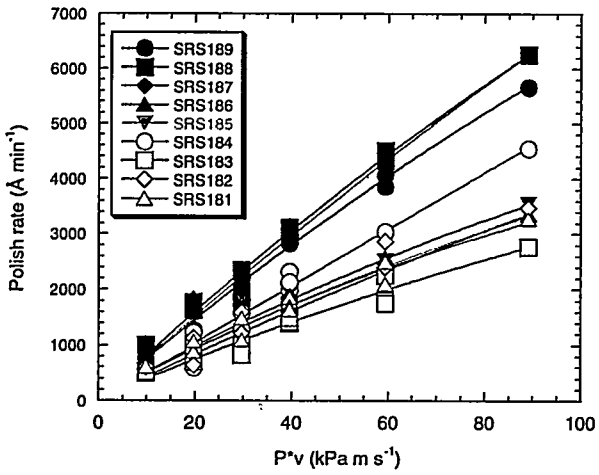

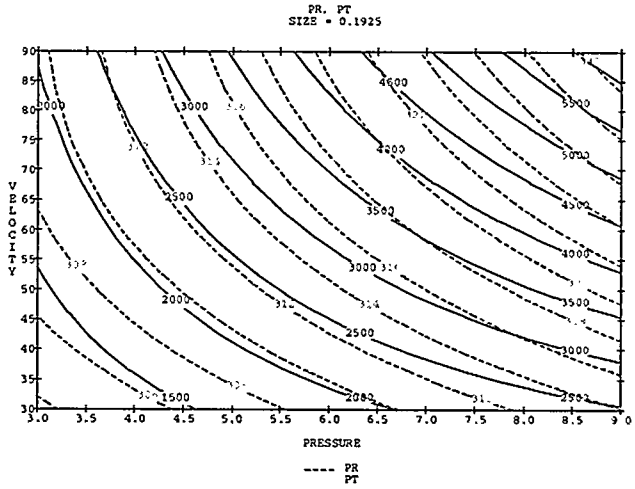

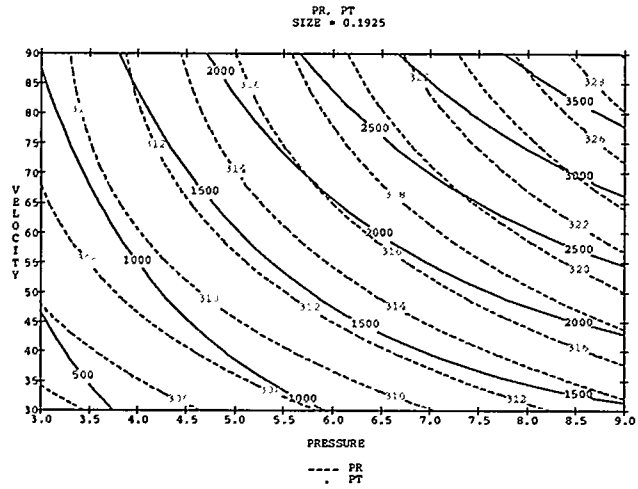

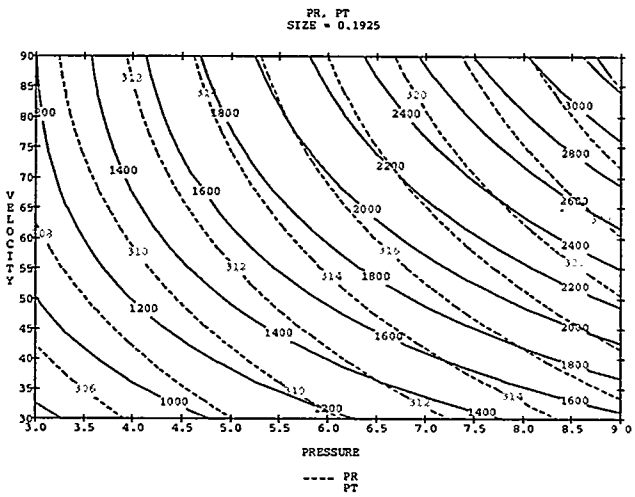

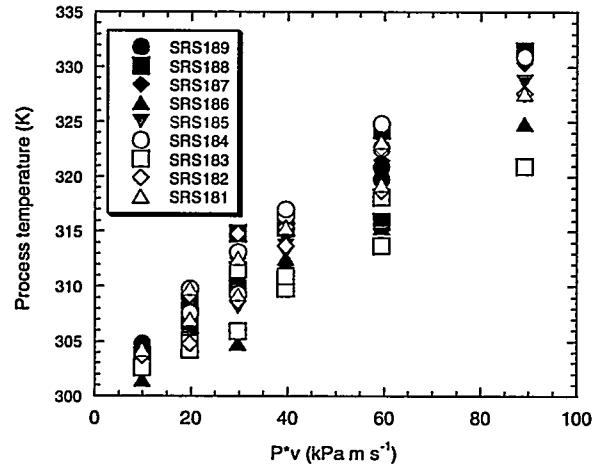

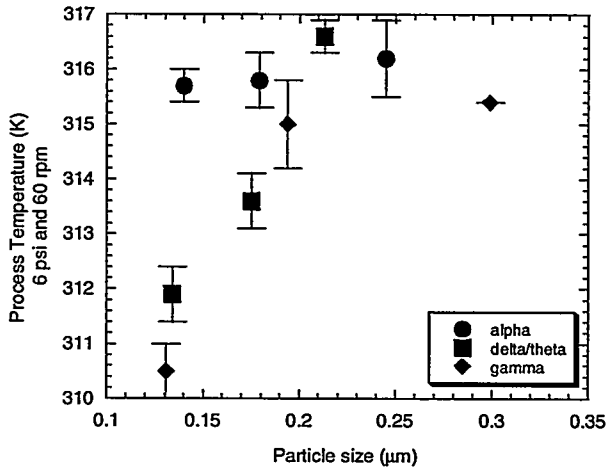

Figure 1 (top left): The polish rate is shown as a function of the alumina type and the product of the pressure and velocity. The labels refer to Ferro Corporation's lot number of each alumina. Figure 2 (top right): the polish rate and process temperature contour plot is shown for alpha alumina. Figure 3 (middle left): the polish rate and process temperature contour plot is shown for delta/theta alumina. Figure 4 (middle right): the polish rate and process temperature contour plot is shown for gamma alumina. Figure 5 (bottom left): the process temperature is shown as a function of the particle phase and the product of the pressure and velocity. The labels refer to Ferro Corporation's lot number of each alumina. Figure 6 (bottom right): the process temperature at the pressure and velocity centerpoint is shown as a function of particle size and phase.

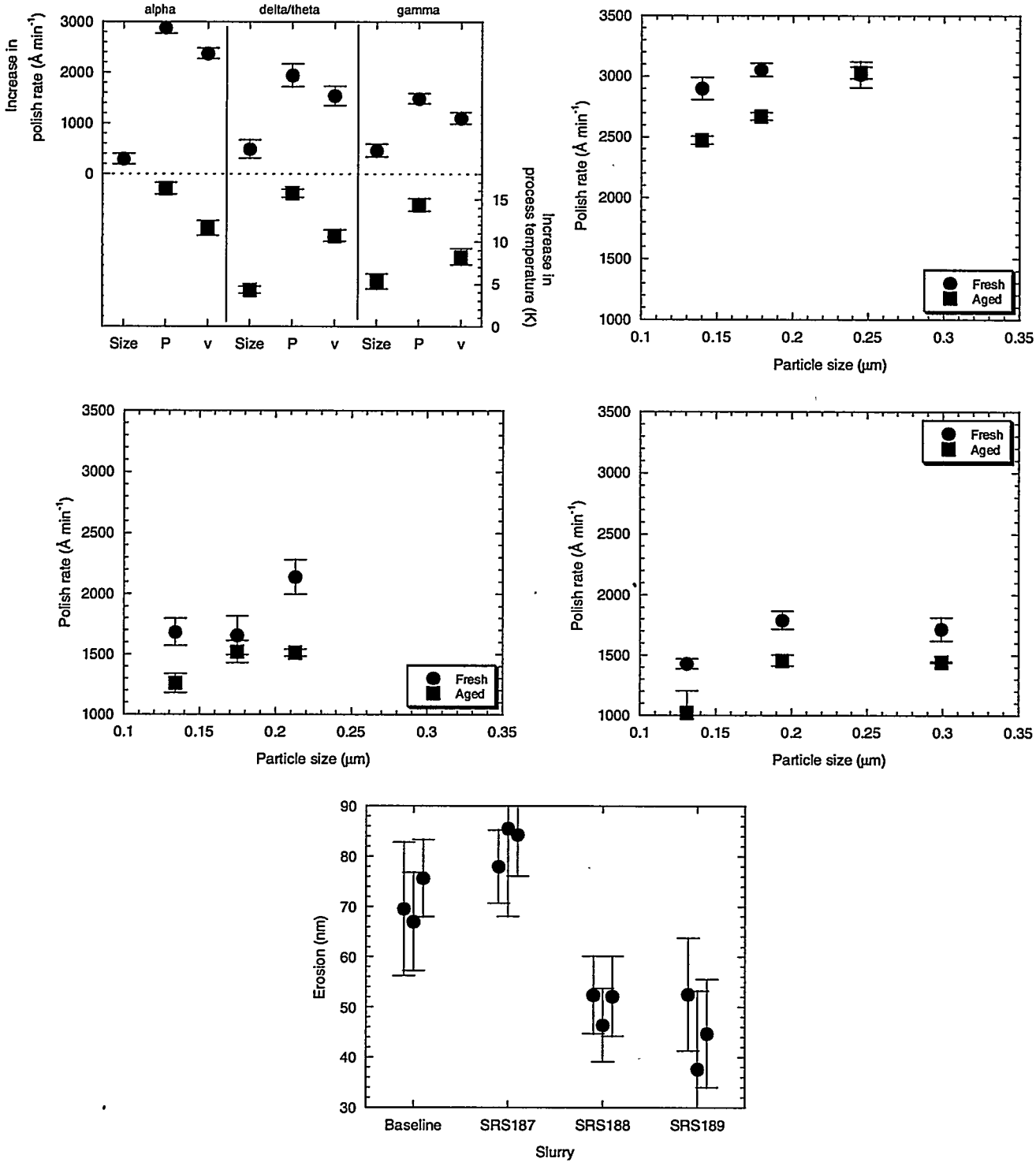

Figure 7 (top left): the main effects of particle size, pressure, and velocity on polish rate and process temperature are shown for each particle phase. The size of the alpha alumina particles was not a significant factor in process temperature. Figure 8 (top right) shows the polish rate difference between the fresh and aged alpha alumina-based slurries. Figure 9 (middle left) shows the polish rate difference between the fresh and aged delta/theta alumina-based slurries. Figure 10 (middle right) shows the polish rate difference between the fresh and aged gamma alumina-based slurries. Figure 11 (bottom) shows the erosion measurements by slurry made using a Digital Instruments VX200 AFM profiler.

Figure 12 shows the AFM images of tungsten plugs post-CMP. The z-axis is 20 μm. The images were acquired using the Digital Instruments VX200 profiling AFM.

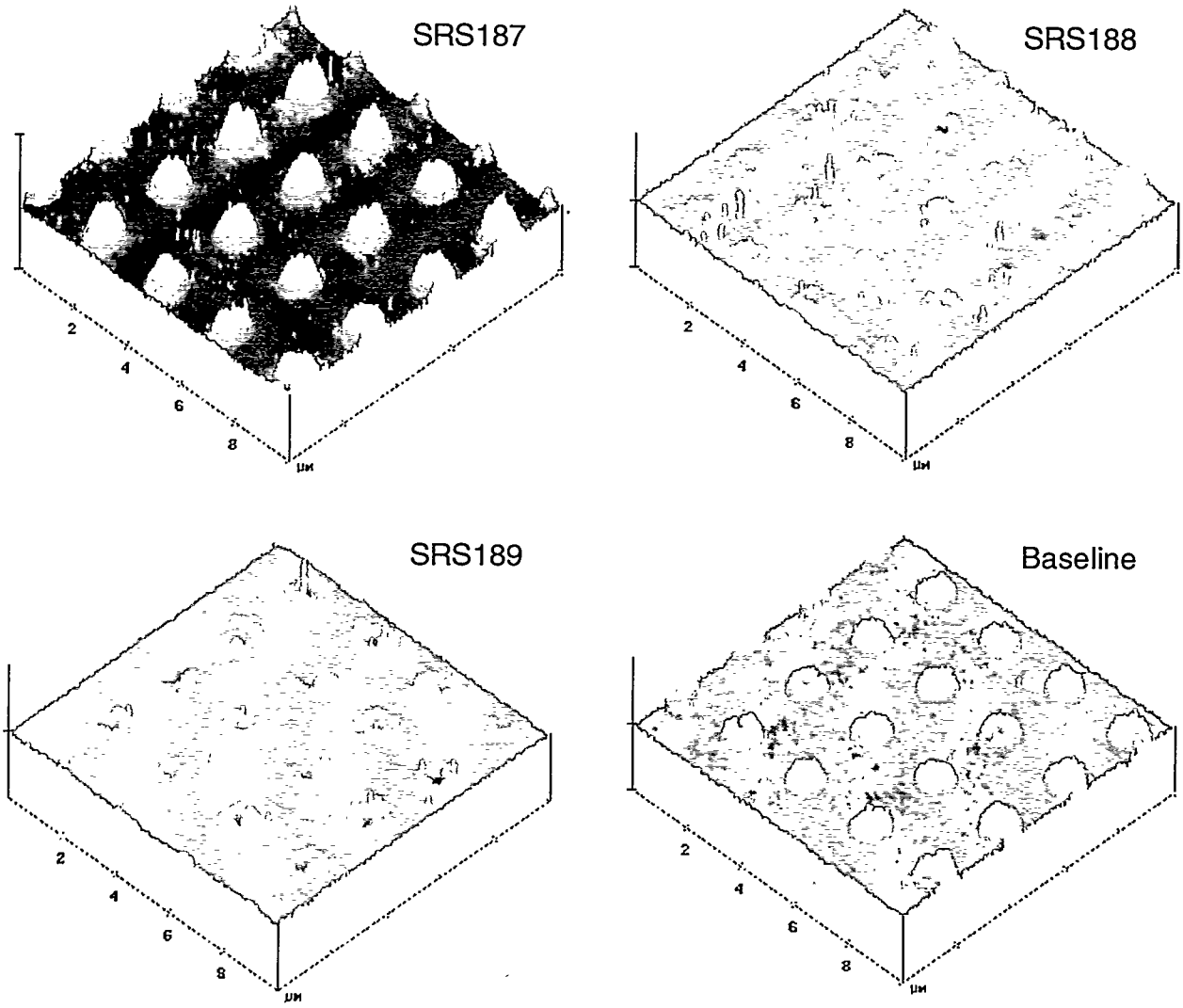

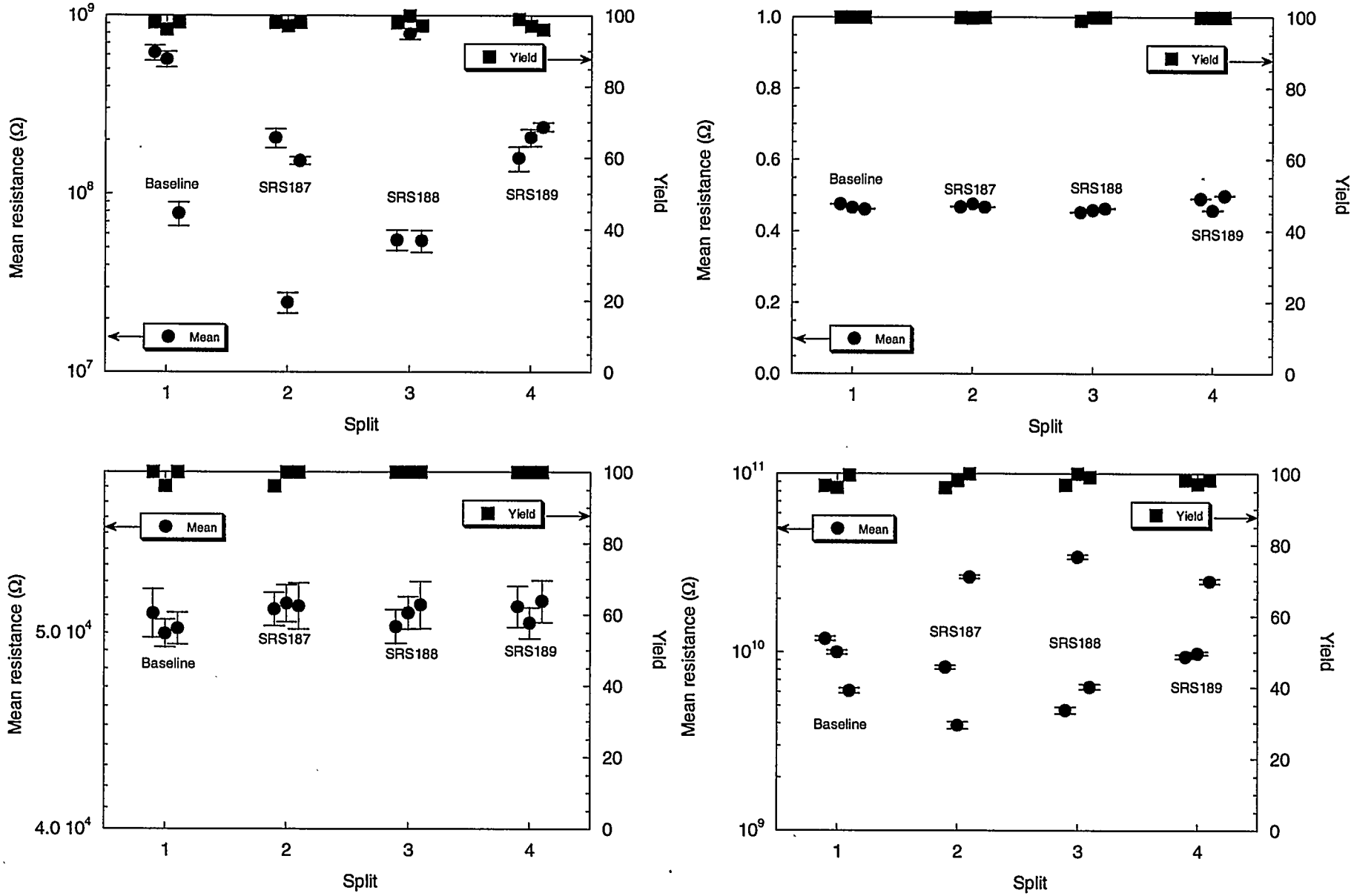

Figure 13 (top left) shows the V1 comb resistance and yield. Figure 14 (top right) shows the V1 to M2 contact resistance. Figure 15 (bottom left) shows the electrical test data from the M2 serpentine structures. Figure 16 (bottom right) shows the electrical test data from the M2 comb structures.